The CIFIST 3D model atmosphere grid

H.-G. Ludwig[1,2], *E. Caffau*[2], *M. Steffen*[3], *B. Freytag*[1,2,4], *P. Bonifacio*[1,2,5]

[1]CIFIST – Marie Curie Excellence Team, [2]GEPI – Observatoire de Paris (France)

[3]Astrophysikalisches Institut Potsdam (Germany), [4]CRAL – ENS-Lyon (France), [5]INAF – OA Trieste (Italy)

Overview. Grids of stellar atmosphere models and associated synthetic spectra are numerical products which have a large impact in astronomy due to their ubiquitous application in the interpretation of radiation from individual stars and stellar populations. 3D model atmospheres are now on the verge of becoming generally available for a wide range of stellar atmospheric parameters. We report on efforts to develop a grid of 3D model atmospheres for late-type stars within the CIFIST Team at Paris Observatory. The substantial demands in computational and human labor for the model production and post-processing render this apparently mundane task a challenging logistic exercise. Here we discuss our approach and experiences gained.

The simulation code. The 3D simulations were performed with the radiation-hydrodynamics code CO^{5}BOLD (Freytag et al. 2002, AN 323, 213).The code solves the time-dependent equations of compressible hydrodynamics coupled to radiative transfer in a constant gravity field in a Cartesian computational domain which is representative of a volume located at the stellar surface. The equation of state takes into consideration the ionization of hydrogen and helium, as well as the formation of H_2 molecules according to Saha-Boltzmann statistics. Relevant thermodynamic quantities – in particular gas pressure and temperature – are tabulated as a function of gas density and internal energy. The multi-group opacities used by CO^{5}BOLD are based on monochromatic opacities stemming from the MARCS stellar atmosphere package (Gustafsson et al. 2008, A&A 486, 951) provided as function of gas pressure and temperature with high wavelength resolution. For the calculation of the opacities solar elemental abundances according Grevesse & Sauval (1998, Space Science Reviews 85, 161) are assumed with the exception of CNO for which values close to the recommendation of Asplund et al. (2005, ASP Conf. Ser. 336, 25) are adopted (specifically, A(C)=8.41, A(N)=7.80, A(O)=8.67).

Model set-up. We typically used a number of $140 \times 140 \times 150$ points for the hydrodynamical grid. The wavelength dependence of the radiation field was represented by 5 multi-group bins in the case of solar metallicity, and 6 bins at sub-solar metallicities. For test purposes we calculated a few models using 12 bins. Starting from a solar standard model, we constructed initial 3D models by scaling existing 3D models according to 1D standard stellar structure models. At given $T_{\rm eff}$ and $\log g$ we kept the computational domain the same for each metallicity. Since the models were intended to serve as atmosphere models for spectral synthesis calculations, a minimum extent of the computational domain to $\log \tau_{\rm Ross} = -6$ was always required. The overall philosophy was to keep the model set-up – in a relative sense – solar-like.

Model calculations and monitoring. The majority of the simulation runs was conducted on a dedicated Linux cluster of 14 double-processor, double-core nodes running one model per node making use of OpenMP parallelization. A main-sequence run is completed in 1–2 months (wall clock time). More CPU demanding giant models were calculated on an IBM SP5 at the Italian CINECA supercomputing center. Running up to 20 hydrodynamical models in parallel made it necessary to facilitate the monitoring of simulation runs. For this purpose we developed an automatic procedure producing diagnostic plots in HTML-format depicting the evolution of the thermal, flux, and oscillatory properties of a model (see **Fig. 1**).

Snapshot selection and auxiliary data. After completion of a model run (see **Fig. 2**), a subset of snapshots is selected for spectral synthesis purposes. The selection is guided by the requirement that the statistics of the sub-sample should closely resemble the statistics of the whole run. In particular the statistics of fluctuation in velocity and emergent flux should be preserved. The selection is done for performance reasons since 3D spectral synthesis calculations are also computationally demanding. The selected data is augmented by basic information about mean model properties, and 1D standard atmosphere models which exactly share the atmospheric parameters with the 3D run.

Grid completeness. At the moment 75 non-solar 3D models have been completed (see **Fig. 3**). On top of this number we calculated a series of solar models and test models with more detailed radiative transfer. Due to a combination of specific needs for projects and computational costs (see **Fig. 4**) most models were produced for dwarfs and sub-giants.

Thoughts for a next generation 3D grid. Higher wavelength and spatial resolution will be evidently a feature of 3D model atmosphere grids of the next generation. A perhaps less obvious property should be a higher degree of homogeneity among the models. A global strategy for designing the computational grid is desirable which takes into consideration the physical structure and constraints given by the numerics. This also relates to the way opacities are grouped. A global strategy ensures an increased differential accuracy of properties among models (e.g., granulation contrast, granular scale, equivalent mixing-length parameter, equivalent width of synthetic lines, etc.). This process will benefit from the already existing 3D models. If grid completeness is important the computational cost of giants necessitates to include them in the production early.

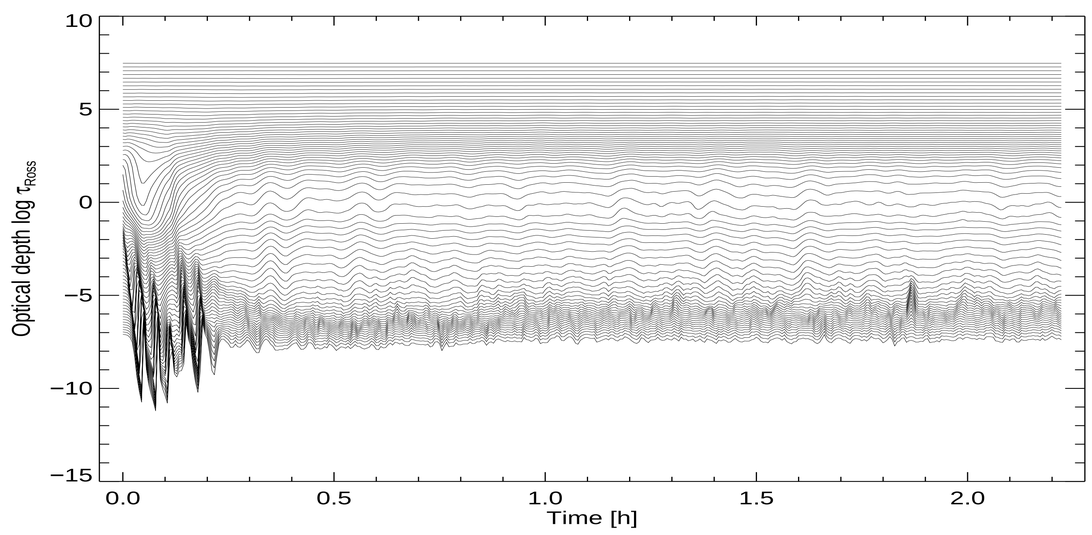

1. Model monitoring ▷ Example of the evolution of the optical depth of each geometrical layer during the run of a metal-poor model ($T_{\rm eff}$=6500 K, logg=4.5, [M/H]=-3). After an initial relaxation phase the model settles into a quasi-stationarity with superimposed oscillations.

2. Model gallery ▷ The panels to the right show typical snapshots of the emergent bolometric intensity from four runs at $T_{\rm eff}$=5000 K, $\log g$=2.5 of different metallicity. The metallicity, the relative RMS intensity contrast of the image and a scale of $10 \times H_{\rm p}^{\rm surf}$ is shown in each frame.

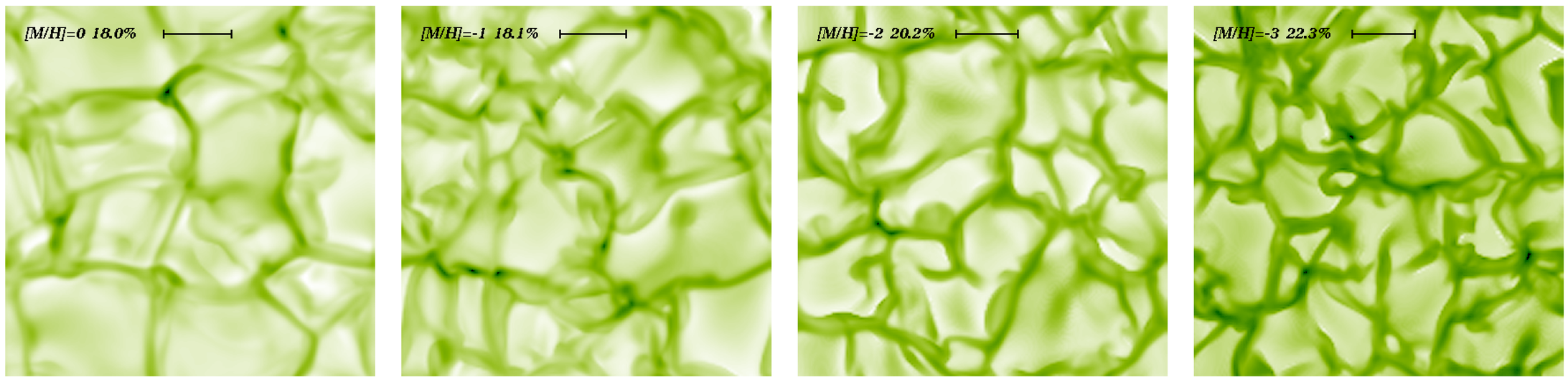

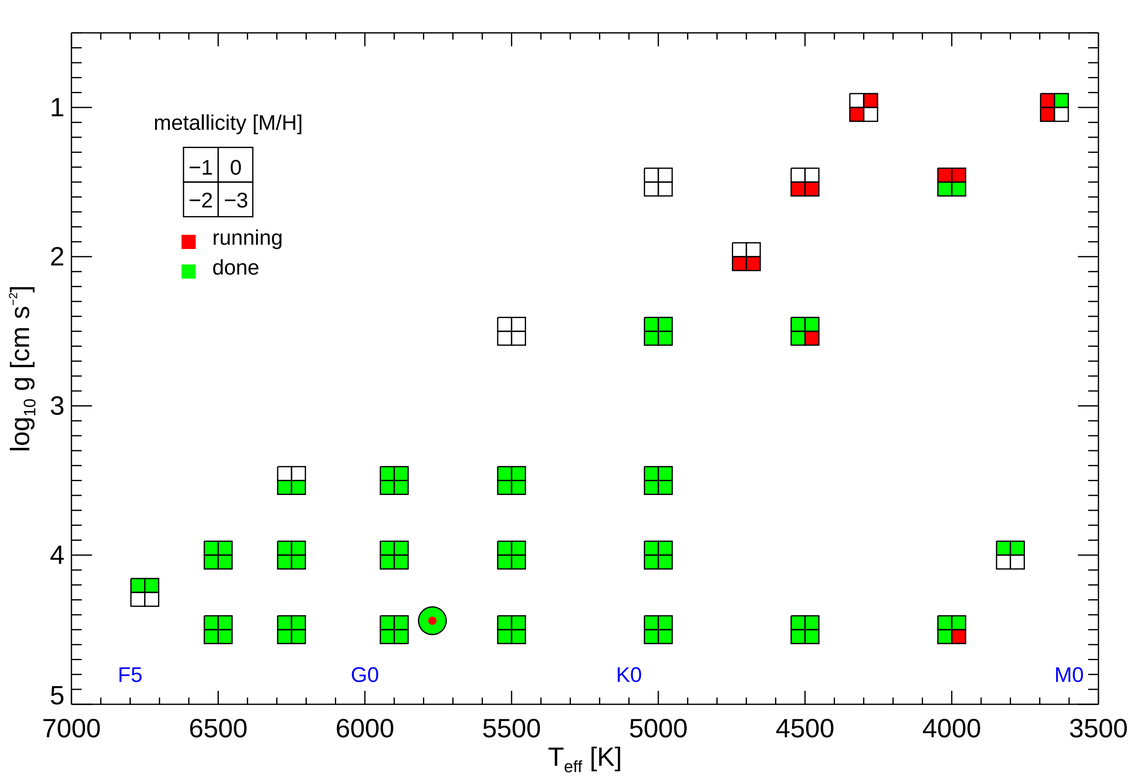

3. Status of model production ▷ Symbols mark the location of a model in the $T_{\rm eff}$-$\log g$-plane. Green color indicates completed model runs, red ongoing calculations. Each square is split into four sub-squares indicating solar, 1/10, 1/100, and 1/1000 of solar metallicity. The solar position is indicated by the round symbol.

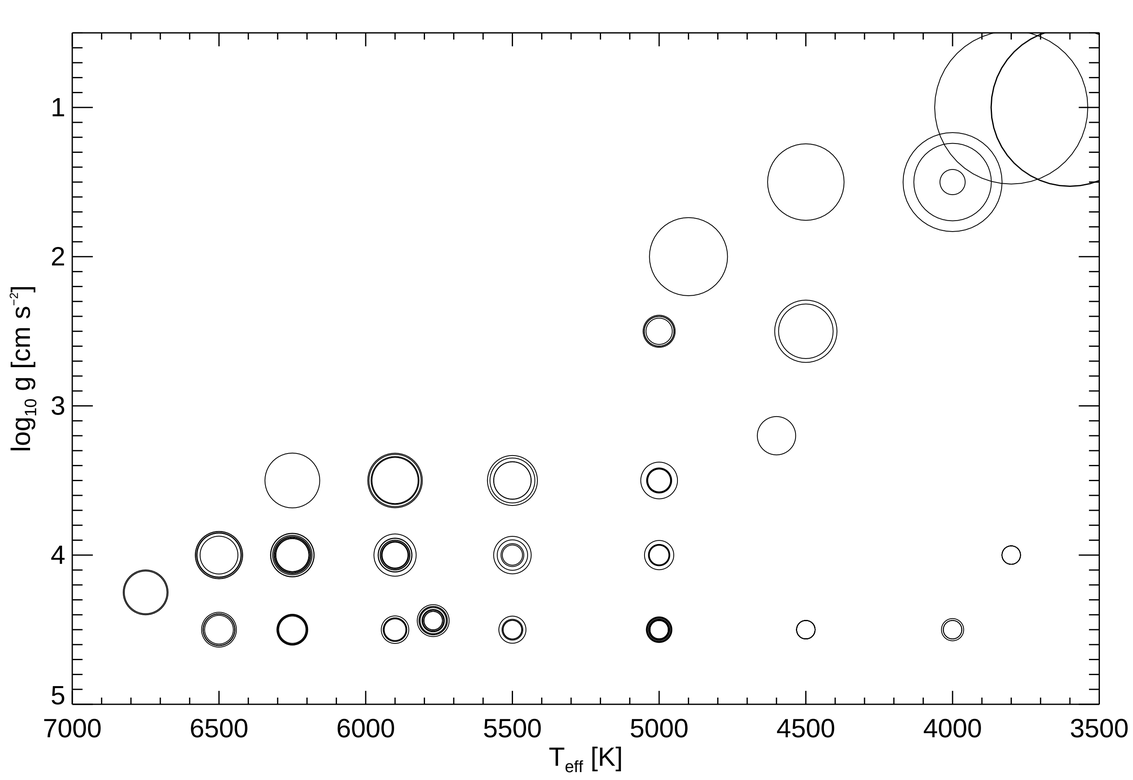

4. Approximate computational model cost ▷ The surface area of a circles depicts the approximate compute time of a model calculation: the symbol diameter is proportional to the quantity $(\Delta t/\Delta t_{\rm CFL})^{-0.5}$ where Δt is the typical timestep, $\Delta t_{\rm CFL}$ the Courant-Friedrichs-Levy time. Metallicity generally plays no dominant role. The computational cost rises significantly towards the red giant branch, and towards higher effective temperatures.